EXPERIMENTAL STUDY OF REINFORCED CONCRETE FRAMES RETROFITTED WITH DUCTILE STEEL FRAMED Y-SHAPED BRACING SYSTEM

by

Yoshiaki NAKANO[1], Fumitoshi KUMAZAWA[2], Hideo KATSUMATA[3], Matsutaro SEKI[4], and Tsuneo OKADA[5]

ABSTRACT

This paper describes seismic performance of 1/10 scaled R/C frames retrofitted with steel framed Y-shaped bracing system, which was developed by the authors. The Y-shaped bracing system consists of a shear panel which can dissipate a large amount of seismic energy due to its inelastic deformation, bracing members which may remain within the elastic range up to large lateral deformations, and a steel frame. In order to investigate the effectiveness of this retrofitting scheme, static loading tests and shaking table tests were carried out and the improved seismic responses are discussed.

1. INTRODUCTION

Recently the installation of steel bracing into existing frames has been widely used for a seismic retrofitting scheme of existing R/C buildings with insufficient seismic capacity. The scheme using steel bracing has a potential advantage over other schemes because of the following reasons:

(1) high strength and stiffness can be provided,

(2) openings to get natural light can be made easily,

(3) the increase in mass associated with the retrofitting is comparatively small and hence foundation cost may be minimized, and

(4) most of the retrofitting work can be performed with prefabricated retrofitting elements and the disruption of occupants can be minimized.

However, most of them were generally focused mainly on the improvement of

---

1) Lecturer, Institute of Industrial Science, University of Tokyo
2) Research Associate, ditto
3) Visiting Research Personnel, ditto, Technical Research Institute, Obayashi Corporation
4) Technical Research Institute, Obayashi Corporation
5) Director and Professor, Institute of Industrial Science, University of Tokyo

stiffness and strength of existing R/C frames.

The authors have developed a seismic retrofitting scheme for existing R/C buildings using ductile steel framed Y-shaped bracing system. This system consists of a shear panel which can dissipate a large amount of seismic energy due to its inelastic deformation, bracing members which is expected to remain within the elastic range up to large lateral deformations, and a steel frame. In order to investigate the effectiveness of this retrofitting scheme, static loading tests and shaking table tests of 1/10 scaled R/C frames retrofitted with the steel framed Y-shaped bracing system were carried out.

2. OUTLINE OF EXPERIMENTS

Five test specimens were constructed, two of which were bare reinforced concrete frames (referred to as F-S and F-D hereafter) and the others were retrofitted with the Y-shaped bracing system (referred to as FB-S, FB-D1 and FB-D2 hereafter) as shown in Fig. 1(a).

Each specimen consisted of two identical one-story and one-bay planar frames and a rigid slab. The R/C frames were designed to fail in columns. The retrofitted specimens were constructed in the following procedures:

(1) casting of concrete for existing frame
(2) setting of bonded anchors into holes precedingly made with tapered pins and cleaned with stiff brush
(3) setting of steel framed bracing system having stud bolts welded around the frame
(4) casting of grouting mortar between the existing frame and steel frame

Concrete and mortar were cast horizontally. The dimension of column was 70 mm x 70 mm and 4 reinforcing bars with a diameter of 4 mm (D4) were placed. Deformed bars with a diameter of 1 mm (D1) which were developed by F. Kumazawa and T. Okada et al.[1] were used for shear reinforcement in columns and two sets of closed hoops were provided at a spacing of 35 mm. The ratio of shear reinforcement p_w was 0.13%. As shown in Fig. 1(b), the retrofitting element installed into the existing R/C frame consisted of a shear panel, bracing members, and a steel frame. The H-shaped shear panel with a stiffening plate, fabricated by welding, was designed so that it could dissipate a large amount of seismic energy due to its inelastic deformation while the bracing members might remain within the elastic range up to large lateral deforma-

tions. The steel frame and the existing R/C frame were jointed by the same technique developed by Y. Yamamoto and S. Kiyota[2] as shown in Fig. 1(c). The joint was spirally reinforced to confine the grouted mortar and effectively transfer shear forces between the welded stud bolts and bonded anchors. Table 1 shows the mechanical properties of material used in the specimens.

Two planar frames and slab were connected rigidly with steel plates and high strength steel rods, and then additional lead blocks were set on both sides of the slab, as shown in Fig. 1(a), to simulate the axial stress in columns of medium-rise R/C buildings. The total weight of the specimen was approximately 6.3 tonf and the axial stress of a column was approximately 25 kgf/cm^2. This value was, however, half of the target due to the space limitation for additional mass.

Table 2 summarizes the experimental program. F-S and FB-S were tested under load reversals. F-D and FB-D1 were subjected to the EW component of Tokachi-Oki Earthquake in 1968 (referred to as "Tokachi EW" hereafter) and FB-D2 to the NS component of Miyagiken-Oki Earthquake in 1978 (referred to as "Miyagi NS" hereafter). Letters "B", "S", and "D" implies "retrofitted with Bracing", "Static loading test" and "Dynamic loading test", respectively.

Before testing, preliminary earthquake response analyses using SDOF system were carried out, and it was confirmed that the shaking table had enough excitation capacity to test the specimens up to failure. Details of the shaking table used in this experiment can be found in Ref. [1].

3. TEST RESULTS

3.1 STATIC LOADING TESTS

In order to investigate the fundamental characteristics of the model structure, specimens F-S and FB-S were tested under load reversals. The load was applied to the rigid slab with two actuators not to distort the specimens, as shown in Fig. 2. Horizontal and vertical displacements of each frame and strains of column reinforcement, steel frames, bracing members, and shear panel were measured.

Fig. 3 shows crack patterns of the specimens when the drift angle of frame, R_F, is 3% (1/33), where R_F is defined by Eq. (1). The observed failure sequence of the specimens is summarized as follows.

o F-S : The longitudinal reinforcement in R/C columns yielded at R_F = 0.5% (1/200) and compressive failure of concrete occurred in the top

of columns at R_F = 3% (1/33). The degradation of lateral load carrying capacity associated with buckling of longitudinal reinforcement in columns and shear cracks across column ends were observed at R_F = 4% (1/25).

o FB-S : The longitudinal reinforcement in R/C columns yielded at R_F = 0.5% (1/200). Flexural-shear cracks were originated at R_F = 1% (1/100) and then widely opened at R_F = 2% (1/50). The shear panel yielded at R_F = 0.25% (1/400) and buckled at R_F = 1% (1/100). The welded portion between flange and web started to fracture at R_F = 2% (1/50) and cracks at welded portion widened and extended during the following loading cycle up to R_F = 3% (1/33). The lateral load carrying capacity degraded gradually during the subsequent repeated loadings and the specimen failed followed by fracture of column shear reinforcement, compressive failure of column concrete, and penetration and widening of cracks. The deformation of FB-S at R_F = 4% (1/25) and the corresponding close-up view of the shear panel are shown in Photo 1.

$$R_F = \delta_F / H_o \qquad (1)$$

where,

R_F : drift angle of the frame
δ_F : average displacement of two planar frames
H_o : clear height of columns (= 350 mm)

As can be seen from the crack patterns of the specimens, the damages in R/C columns of FB-S were observed apart from column ends because the critical section shifted due to the presence of steel frame and gusset plate for the retrofitting bracings while they were mainly concentrated near the critical section of columns in F-S. Large slippage was not observed between the existing R/C frame and retrofitting steel frame although cracks were slightly observed in grouting mortar. As expected in the design of the specimens, the bracing members remained within the elastic range except for the final loading stage up to failure.

Fig. 4 shows load vs. displacement relationship of the specimens. The retrofitted specimen FB-S exhibits improved response in terms of strength, stiffness, and energy dissipation. The ultimate capacity of FB-S is approximately 5 times as much as that of F-S. Furthermore, the retrofitted specimen shows a stable and large energy dissipation up to the drift angle of 3%

(1/33). It should be noted that FB-S shows a larger energy dissipation even when the displacement of frame is relatively small. This is because the deformation of bracing system is mainly attributed to the shear deformation of the panel as shown in Photo 1, and hence the drift angle of the shear panel (R_P) is 5.8 times that of the frame (R_F) and the shear panel experiences a large inelastic deformation even when the overall displacement of the frame is small in the early loading stage.

Fig. 5 shows cumulative displacement (δ_{cum}) vs. cumulative hysteretic energy dissipation (E_{cum}) relationship of F-S and FB-S specimen, where δ_{cum} and E_{cum} are defined in Eqs.(2) and (3), respectively. In this Figure, the cumulative energy dissipation of the shear panel is also compared with overall energy dissipation of the frame. As stated earlier, the bracing members remained within the elastic range except for the final loading stage, and hence the load carried by the shear panel is evaluated from the axial forces of bracing members which can be calculated from the measured strains with the assumption of pin-connection at the shear panel and bracing members. It can be seen from this Figure that the energy dissipation of FB-S is 8 times as much as that of F-S and that the contribution of the shear panel to the total energy dissipation is approximately 75% after the loading cycle with maximum drift of 3% (1/33) as indicated with "o" in the Figure.

$$\delta_{cum} = \Sigma |\Delta \delta_{Fi}| \quad (2)$$

$$E_{cum} = \Sigma \Delta E_i \quad (3)$$

where,

δ_{cum} : cumulative displacement

$\Delta \delta_{Fi}$: increase or decrease of displacement at i-th loading step

E_{cum} : cumulative hysteretic energy dissipation calculated from the area enclosed by the hysteretic loop

ΔE_i : increase or decrease of hysteretic energy dissipated during i-th loading step

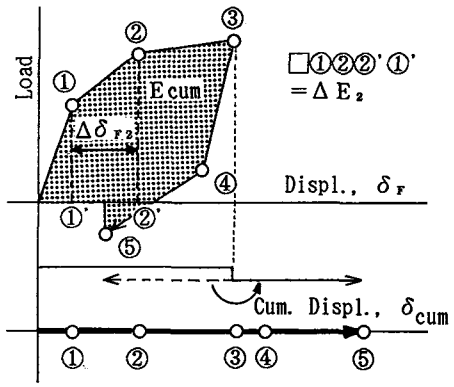

In order to investigate the effects by downsizing of the specimens, test results were also compared with those of 1/3 scaled model which was retrofitted by the similar scheme to 1/10 scaled specimen FB-S and tested previously under load reversals[3]. Fig. 6 shows normalized cumulative displacement $\overline{\delta}_{cum}$

vs. normalized energy dissipation $\bar{E}_{cum}$ relationship of FB-S and 1/3 scaled specimen, where $\overline{\delta}_{cum}$ and $\bar{E}_{cum}$ are defined by Eqs. (4) and (5), respectively. It is seen from this Figure that the tendency of energy dissipation is similar in both specimens, and the downsizing effect is not found in the hysteretic energy characteristics.

$$\overline{\delta}_{cum} = \delta_{cum} / Ho \quad (4)$$

$$\bar{E}_{cum} = E_{cum} / (Q_{max} \cdot Ho) \quad (5)$$

where,

$\overline{\delta}_{cum}$: cumulative displacement normalized with respect to the height of the specimen, i.e. cumulative drift angle

δ_{cum} : cumulative displacement defined by Eq. (2)

Ho : clear height of column (350 mm for 1/10 model, 900 mm for 1/3 model)

$\bar{E}_{cum}$: cumulative hysteretic energy dissipation normalized with respect to the height and lateral load carrying capacity of the specimen

E_{cum} : cumulative hysteretic energy dissipation defined by Eq. (3)

Q_{max} : lateral load carrying capacity of the specimen measured during tests

3.2 Shaking Table Tests

In order to investigate the dynamic performance of the model structure, specimens F-D and FB-D1 were subjected to the Tokachi EW and FB-D2 to the Miyagi NS. All three specimens were excited uniaxially in the longitudinal direction as shown in Fig. 7.

Table 3 shows the law of similarity. As stated previously, the axial stress of 25 kgf/cm^2 in a column of the specimens was half of the target value. The natural period of the specimen, therefore, was actually $1/\sqrt{2}$ times of the target; i.e. the actual scaling factor of the natural periods was $1/\sqrt{20}$. Hence, the time scale of the original record was "compressed" to $1/\sqrt{20}$ in Runs 0 through 5 in accordance with the law of similarity while the compressed accelerogram was elongated by $\sqrt{2}$ times (i.e. $1/\sqrt{10}$ of the original) to observe the ultimate failure mechanism of the specimens in Runs 6 and 7. It should be also noted that the input acceleration level to the actual structures corresponds to 1/2 times that to the specimens because the weight of the specimen is half of the target. The compressed acceleration data were then modified through a digital filter shown in Fig. 8 to truncate the frequency contents higher than 30 Hz and lower than $0.1x/\sqrt{20}$ Hz. In Fig. 9 the magnification factors of response acceleration with 2%, 5%, and 10% of critical damping to Tokachi EW and Miyagi NS are shown with respect to three different time scales; i.e. the original time scale, $1/\sqrt{10}$ ($=\sqrt{2} \times 1/\sqrt{20}$) of the original in

Runs 6 and 7, and $1/\sqrt{20}$ of the original in Runs 0 through 5.

At first, these three specimens were subjected to a low amplitude of acceleration, and then the intensity was gradually increased in subsequent test runs. Table 4 summarizes the input acceleration. In each test run, the maximum input acceleration was scaled so that the ratio of the yielding strength Ky' to the maximum input acceleration Kg should be equal among specimens: Ky'/Kg = 16 in Run 0, 8 in Run 1, 4 in Run 2, 2 in Run 3, and 1 in Runs 4 through 7, respectively. The values of Ky' were determined from the static loading test results for FB-D1 and FB-D2 while it was determined from the calculated yielding capacity Qy=1.66 tonf because F-S was tested after the remaining four specimens, FB-S, FB-D1, FB-D2 and F-D, due to the testing schedule convenience.

Three components of response acceleration, horizontal and vertical response displacements of each frame and strains of longitudinal reinforcement, steel frame, bracing members, and shear panel were measured at the time interval of 1/200 secs.

Fig. 10 shows crack patterns of the specimens after Run 5 for F-D and FB-D2 and after Run 6 for FB-D1, where the maximum drift angle R_F is approximately 3%. Table 5 shows the maximum response results in each test run. The responses observed during tests are summarized as follows.

- o FB-D1 : No cracks (Run 0), yielding of the shear panel (Run 3), many flexural cracks and yielding of the longitudinal reinforcement and steel frame (Run 4), many shear cracks, residual deformation in the shear panel, and cracks in joint mortar along the column (Run 5), compressive failure in the column and penetration of cracks in the shear panel (Run 6) were observed, respectively.
- o FB-D2 : No cracks (Run 0), yielding of the shear panel (Run 2), many shear cracks in the columns, yielding of the longitudinal reinforcement and steel frame, residual deformation in the shear panel, and cracks in joint mortar along the column (Run 4), compressive failure and shear failure in the column and penetration of cracks in the shear panel (Run 5) were observed, respectively.
- o F-D : Flexural cracks (Run 0), yielding of the longitudinal reinforcement (Run 4), compressive failure at column ends (Run 6), and propagation of cracks and compressive failure in the columns (Run

7) were observed, respectively.

As can be seen from the comparison of Fig. 3 and Fig. 10, crack patterns of FB-D1 and FB-D2 were similar to those of FB-S while F-D sustained less but wider cracks than F-S. The shear panel of FB-D1 and FB-D2 were, however, more severely damaged than that of FB-S although the maximum displacements were similar among these three specimens. This resulted mainly from the larger seismic energy input into FB-D1 and FB-D2, because they had been already subjected to preceding test runs and hence the cumulative displacement of FB-D1 and FB-D2 was much larger than that of FB-S.

Fig. 11 shows the story shear force vs. response displacement relationship, where the shear force is calculated by the product of the observed response acceleration and the weight of the superstructure. The shape of response hysteretic loops varies depending on the input accelerogram, i.e. FB-D1 and F-D subjected to Tokachi EW show an asymmetrical response pattern between the positive and negative displacement zones while FB-D2 subjected to Miyagi NS shows a symmetrical pattern. However, as was seen in the results of static loading tests, the retrofitted specimens FB-D1 and FB-D2 show better seismic performance in terms of strength, stiffness and hysteretic energy and the shape of the hysteretic loops of each specimen shown in Fig. 11 are generally similar to those of corresponding specimens subjected to static loadings shown in Fig. 4.

Fig. 12 shows the relationship between maximum response displacement and strength ratio Ky/Kg, where Ky signifies maximum response acceleration of the specimen and Kg maximum input acceleration, respectively. This Figure shows that the response displacements of the retrofitted specimens FB-D1 and FB-D2 are reduced to 1/4 of those of the bare frame specimen F-D when the specimens are subjected to the same level of seismic forces, i.e. Ky/Kg. This better seismic performance results mainly from the improved seismic energy dissipation capacity of the shear panel.

4. CONCLUDING REMARKS

In order to investigate the effectiveness of the retrofitted scheme which was developed by the authors, static loading tests and shaking table tests were carried out using 1/10 scaled R/C model. The conclusions can be summarized as follows.

(1) The Y-shaped bracing system installed within an existing R/C frame can

improve the seismic response in terms of strength, stiffness, and hysteretic energy. The ultimate strength of the retrofitted frame was 5 times and the hysteresis energy dissipation was 8 times as much as that of the original bare frame. The contribution of the shear panel to the total energy dissipation was approximately 75 % after the loading cycle with maximum drift of 3%.

(2) The tendency of energy dissipation of 1/10 scaled specimen and 1/3 scaled specimen was similar, and the significant difference due to the downsizing was not found in the hysteretic energy characteristics of the retrofitted specimens.

(3) Hysteresis characteristics and failure mode of the specimens subjected to the dynamic excitation were similar to those of corresponding specimens subjected to the static loadings except that less but wider cracks were observed during the shaking table tests in the original bare specimen.

(4) Seismic performance was improved by the better energy dissipation capacity of the shear panel in the steel framed bracing system installed within an existing R/C frame and the response displacements of the retrofitted frames were approximately 1/4 of those of the bare frame when subjected to the same level of seismic forces.

ACKNOWLEDGEMENT

This experiment was carried out under the cooperative research project between Institute of Industrial Science, the University of Tokyo, and Obayashi Corporation. The authors are gratefully acknowledged to Dr. Toshikazu TAKEDA, director of Technical Research Institute of Obayashi Corporation and Dr. Yoshiro KOBATAKE, manager of the structural construction research laboratory, Technical Research Institute of Obayashi Corporation, for their helpful suggestions.

REFERENCES

[1] T. Okada, F. Kumazawa and others : "Shaking Table Tests of Reinforced Concrete Small Scaled Model Structures," Bulletin of ERS, No. 22, pp. 3-12, march 1989.

[2] Y. Yamamoto and S. Kiyota : "Experimental Study on Strengthening of Reinforced Concrete Buildings (part 2. Strengthening by Steel Systems)," Proc. of the 29th Structural Engineering Symposium, AIJ and JSCE, pp. 91-98, 1983. (in Japanese)

[3] H. Katsumata, M. Seki, F. Kumazawa and T. Okada : "Retrofit method of Existing Reinforced Concrete Structures by Ductile Steel Braces," Transactions of the Japan Concrete Institute, Vol. 11, pp. 285-292, December 1989.

Table 1 : Mechanical Properties of Material

(1) Strength of Concrete (in average, kgf/cm²)

F-S , FB-S		F-D, FB-D1, D2		Location
σ_c	σ_t	σ_c	σ_t	
359.2	24.4	378.9	47.5	beams and columns*
657.6	--	556.0	26.9	grouting at joints

σ_c : compressive strength σ_t : tensile strength

* W/C=65% air content=7%
AE (Air-Entraining) water reducing agent was used.

(2) Strength of Anchors (in average, kgf/cm²)

σ_{max}*	Note
290.8	1)Holes where anchors were placed were cleaned with stiff brush. 2)3 out of 4 tested anchors failed in anchor bolt. The remaining was concrete cone failure.

* : pull-out strength of bonded anchors

(3) Strength of Steel (in average, kgf/cm²)

(1) E_s	(2) σ_y	(3) ε_y	(4) σ_{max}	(5) σ_B	(6) ε_B	Location
1.96	4045	0.4025	4514	0.4209	11.7	bracing members
2.09	2556	0.1309	3759	0.2468	31.7	main reinforcement(D4) in column
--	3320*	--	3808	--	--	shear reinforcement(D1) in column
2.10	1842*	--	3017	0.2048	44.8	web of shear panel
2.09	3229	0.1642	4337	0.3453	32.1	steel frame
2.09	2471*	--	3562	0.2565	37.1	flange and stiffener of shear panel

(1)Young's modulus [x10⁶, kgf/cm²] (2)yielding strength [kgf/cm²] (3)strain at yielding [%]
(4)maximum strength [kgf/cm²] (5)breaking strength [kgf/cm²] (6)elongation at breaking [%]
(* indicates 0.2 % offset value.)

Table 2 : Summary of Experimental Program

Specimens	Retrofitting Scheme	Loading Type
(1) F-S	Original Bare Frame	Static Loading
(2) FB-S	Retrofitted Frame	
(3) F-D	Original Bare Frame	Tokachi EW
(4) FB-D1	Retrofitted Frame	
(5) FB-D2		Miyagi NS

[Note]
"Tokachi EW" signifies the EW component of Tokachi-Oki Earthquake recorded in 1968.
"Miyagi NS" signifies the NS component of Miyagiken-Oki Earthquake recorded in 1978.

Table 3 : Law of Similarity

	Target	Actual
Length	1/10	1/10
Stress	1	1*1
Strain	1	1
Time	$1/\sqrt{10}$	$1/(\sqrt{10}\times\sqrt{2})$
Weight*2	$1/10^2$	$1/(10^2\times 2)$
Deformation	1/10	1/10
Drift Angle	1	1
Acceleration	1	2
Inertia Force	$1/10^2$	$1/10^2$
Shear Coeff.	1	2
Natural Period	$1/\sqrt{10}$	$1/(\sqrt{10}\times\sqrt{2})$

*1 : Axial stress is half of the target value. *2 : Total weight including additional lead blocks

Table 4 : Maximum Input Acceleration

Run Steps	Maximum Input Acceleration (gal)			
	Target	Observed (Max. and Min. Value)		
		FB−D1	FB−D2	F−D
Run 0	123 (20)	129 -138	142 -101	26 -24
Run 1	245 (40)	248 -264	300 -219	48 -41
Run 2	490 (80)	527 -554	524 -433	92 -72
Run 3	980 (160)	1069 -945	1092 -878	164 -113
Run 4	1960 (320)	2381 -1736	2150 -1935	352 -277
Run 5	1960 (320)	2341 -1794	2245 -1938	362 -318
Run 6	1960 (320)	2159 -1825	-- --	367 -369
Run 7	1960 (320)	-- --	-- --	408 -400

※ Values in parentheses are the target for the specimen F-D. The time scale in Runs 6 and 7 was compressed to $1/\sqrt{10}$ of the original while $1/\sqrt{20}$ in Runs 0 through 5. The symbol "--" in Runs 6 and 7 indicates that the test was not carried out.

Table 5 : Maximum Responses

Run Steps	FB−D1			FB−D2			F−D		
	C_B	R_F [in %]	Ky/Kg	C_B	R_F [in %]	Ky/Kg	C_B	R_F [in %]	Ky/Kg
Run 0	0.15	1/7450 [0.01%]	14.82	0.15	1/7450 [0.01%]	14.93	0.05	1/3020 [0.03%]	18.84
Run 1	0.28	1/3680 [0.03%]	7.77	0.32	1/3470 [0.03%]	7.07	0.08	1/1250 [0.08%]	10.11
Run 2	0.60	1/1550 [0.07%]	3.69	0.56	1/1810 [0.06%]	4.05	0.18	1/550 [0.18%]	5.24
Run 3	1.18	1/532 [0.19%]	1.91	1.17	1/571 [0.18%]	1.94	0.27	1/294 [0.34%]	2.95
Run 4	2.02	1/126 [0.79%]	0.86	2.16	1/54 [1.85%]	0.99	0.39	1/89 [1.12%]	1.37
Run 5	2.09	1/66 [1.52%]	0.87	1.95	1/32 [3.13%]	0.95	0.42	1/36 [2.78%]	1.33
Run 6	2.01	1/36 [2.77%]	0.95	---			0.49	1/21 [4.76%]	1.31
Run 7	---			---			0.41	1/14 [7.14%]	1.18

C_B : maximum story shear coefficient, R_F : maximum inter-story drift angle of frame(See Eq. (1))
Ky/Kg : yielding strength ratio (Ky and Kg are maximum response acceleration and maximum input acceleration in terms of gravity during each Run, respectively.)
※ The symbol "---" in Runs 6 and 7 indicates that the test was not carried out.

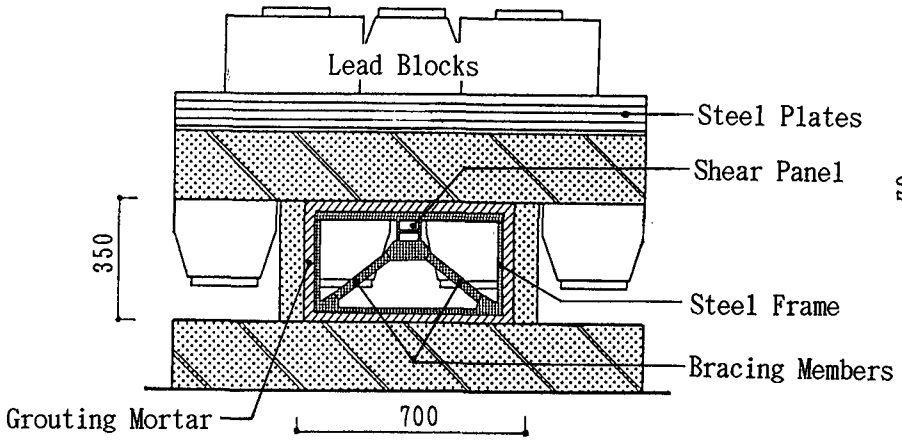

(a) Outline of Retrofitted Specimen

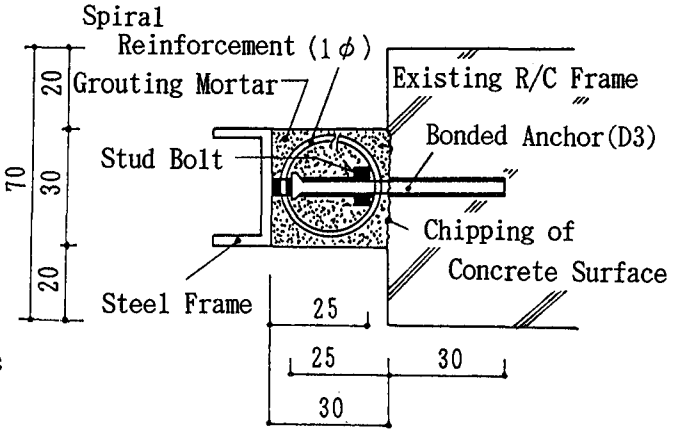

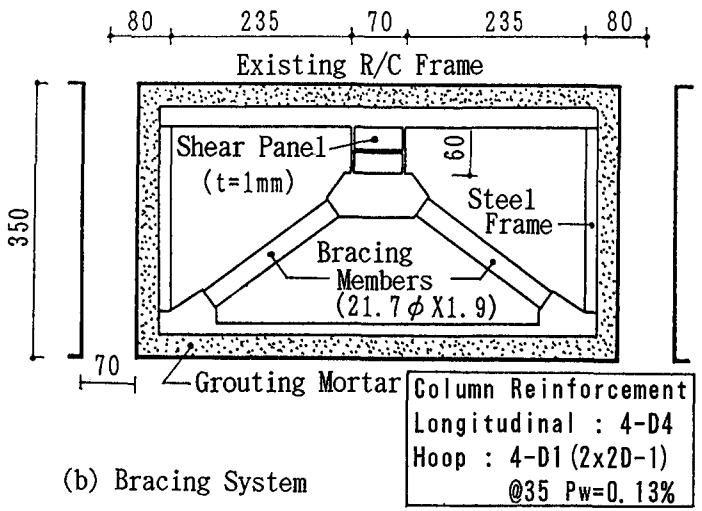

(b) Bracing System

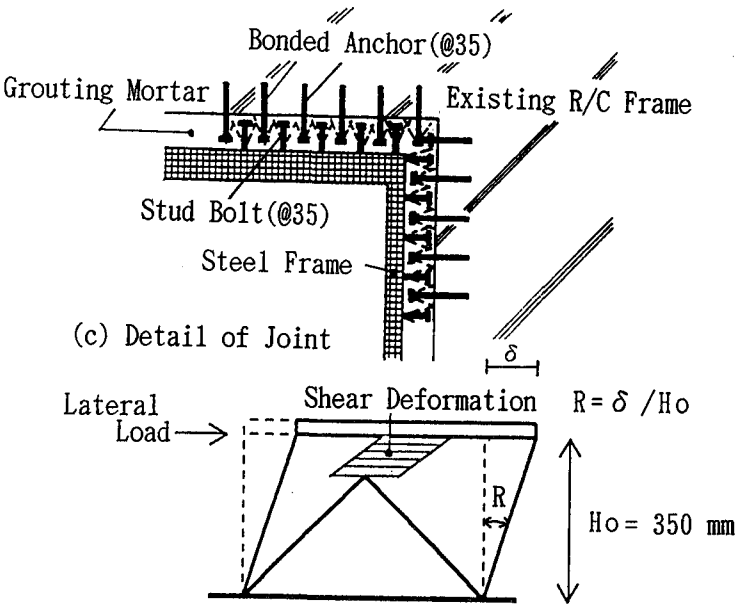

(c) Detail of Joint

Fig. 1 : Dimensions of Retrofitted Specimen (unit : mm)

* Additional lead blocks are not shown in this Figure.

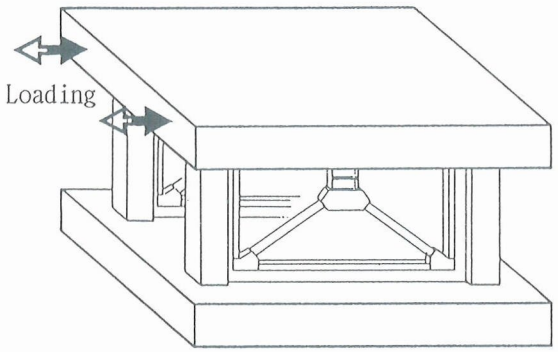

Fig. 2 : Loading Method of Static Loading Tests

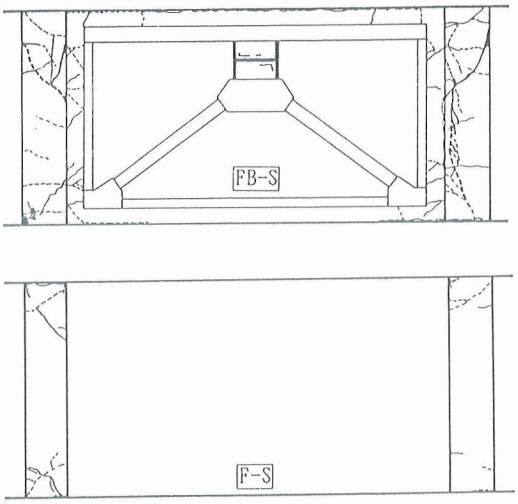

Fig. 3 : Crack Patterns of F-S and FB-S (R_F=3%)

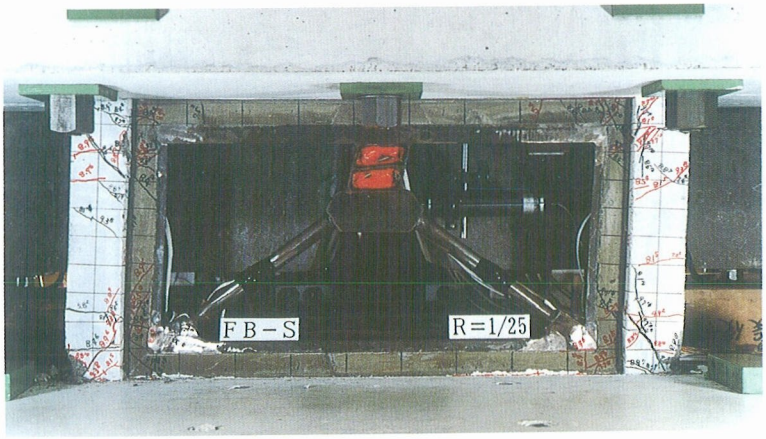

(a) General View

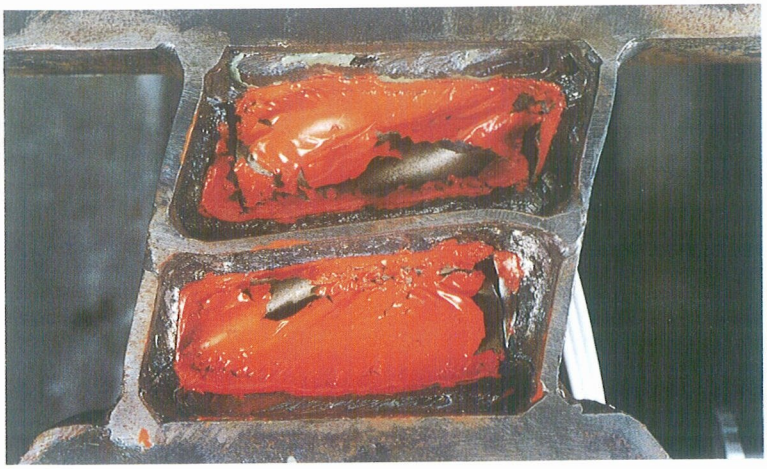

(b) Close-up View of Shear Panel

Photo 1 : Deformation of FB-S (R_F=4%)

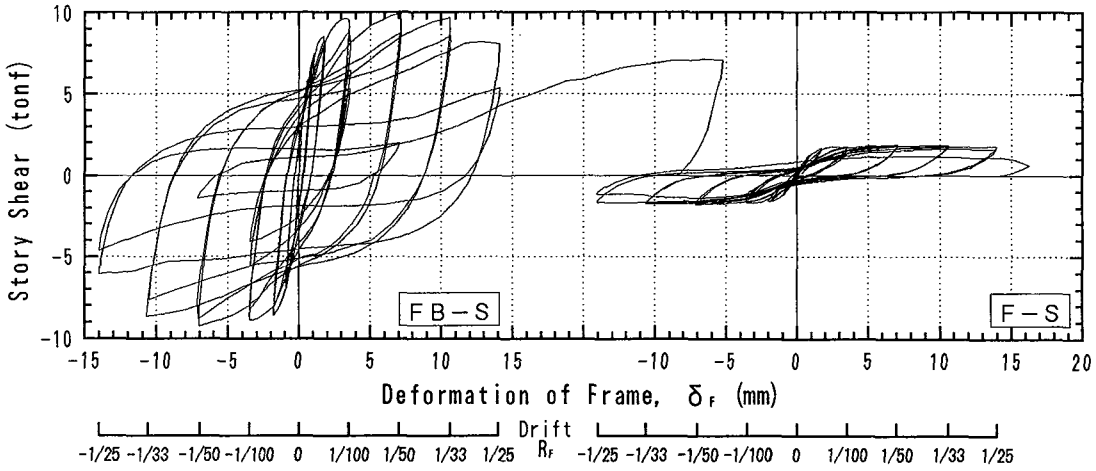

Fig. 4 : Load vs. Displacement Relationship

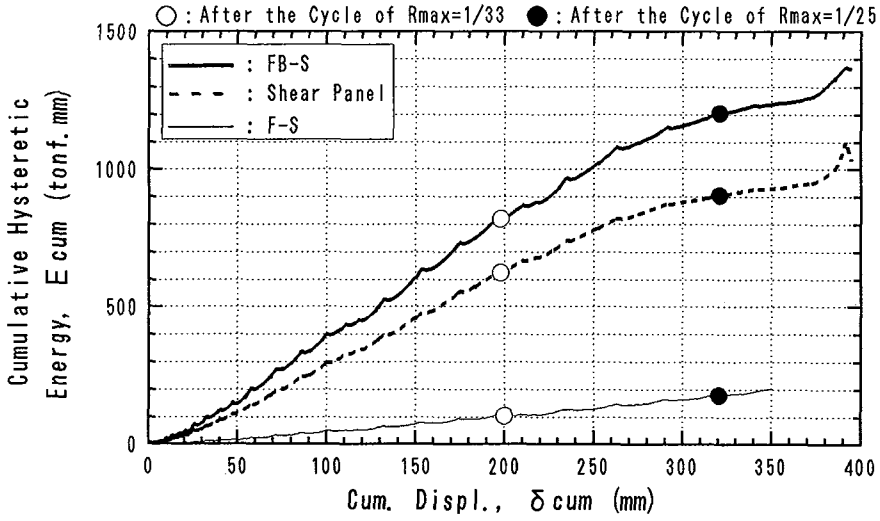

Fig. 5 : Cum. Displacement vs. Cum. Hysteretic Energy

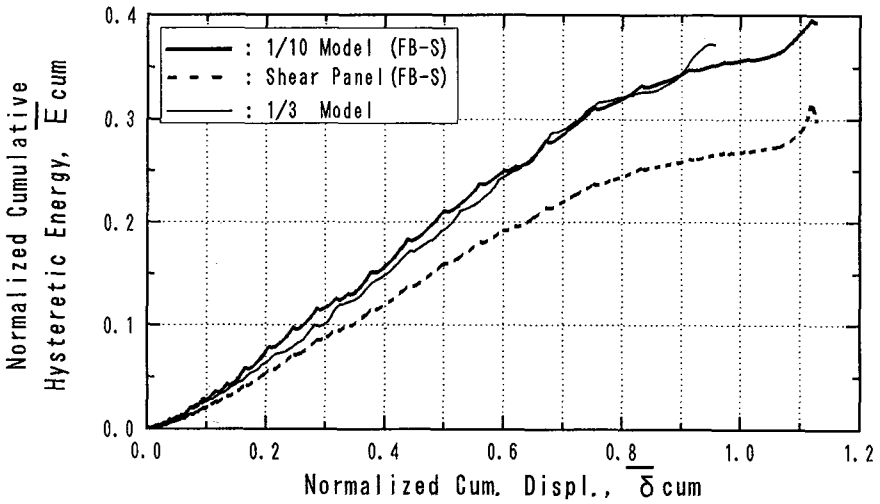

Fig. 6 : Comparison of Normalized Cumulative Hysteretic Energy

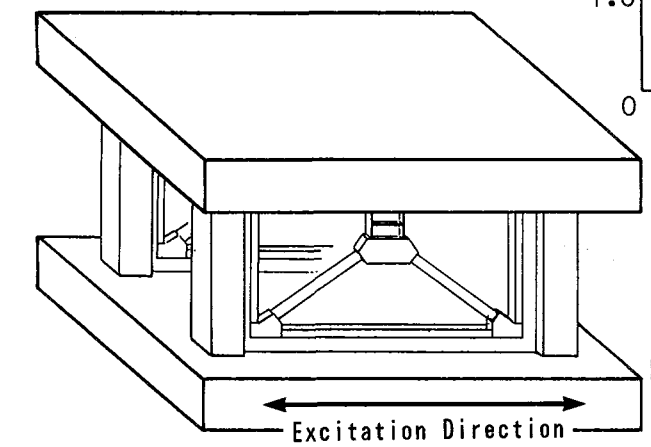

Fig. 7 : Excitation Direction of Shaking Table Tests

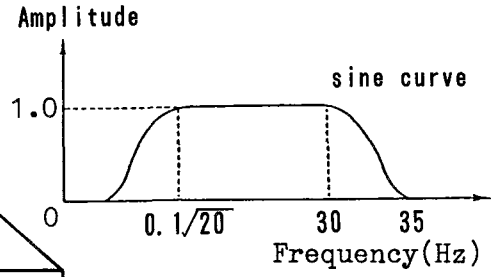

Fig. 8 : Digital Filter

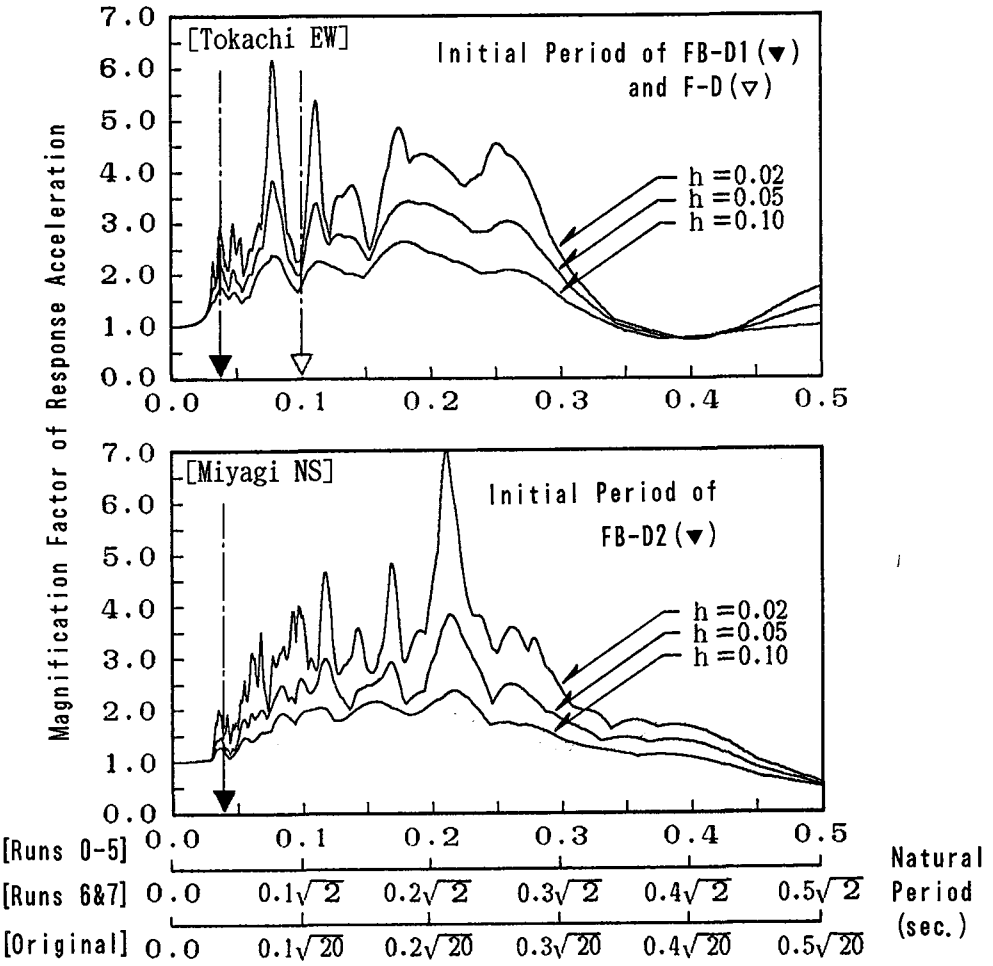

Fig. 9 : Response Acceleration Magnification Spectra of Input Acceleration

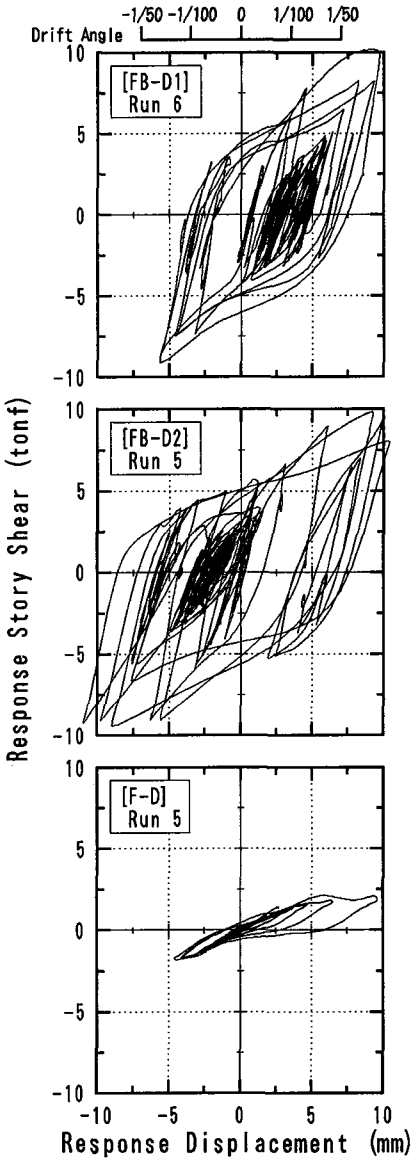

Fig. 11 : Response Characteristics

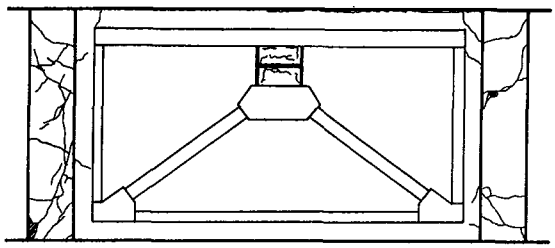

[FB-D1] After Run 6 R_{max}=1/36

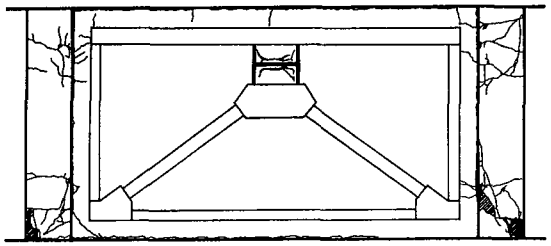

[FB-D2] After Run 5 R_{max}=1/32

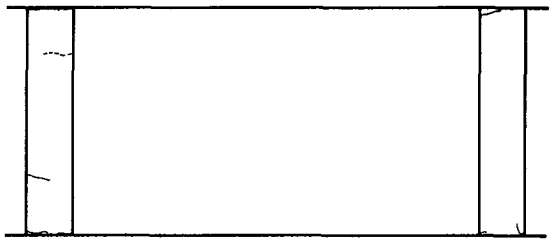

[F-D] After Run 5 R_{max}=1/36

Fig. 10 : Crack Patterns Due to Shaking Table Tests

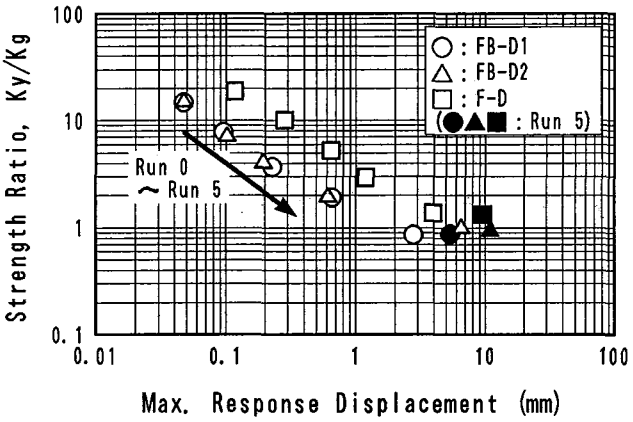

Fig. 12 : Max. Response Displacement vs. Strength Ratio, Ky/Kg